# *Investigation of Er-doped $Sc_2O_3$ transparent ceramics by positron annihilation spectroscopy*

**L. G. Jacobsohn, K. Serivalsatit, C. A. Quarles & J. Ballato**

**Journal of Materials Science**
Full Set - Includes `Journal of Materials Science Letters'

ISSN 0022-2461
Volume 50
Number 8

J Mater Sci (2015) 50:3183-3188
DOI 10.1007/s10853-015-8881-8

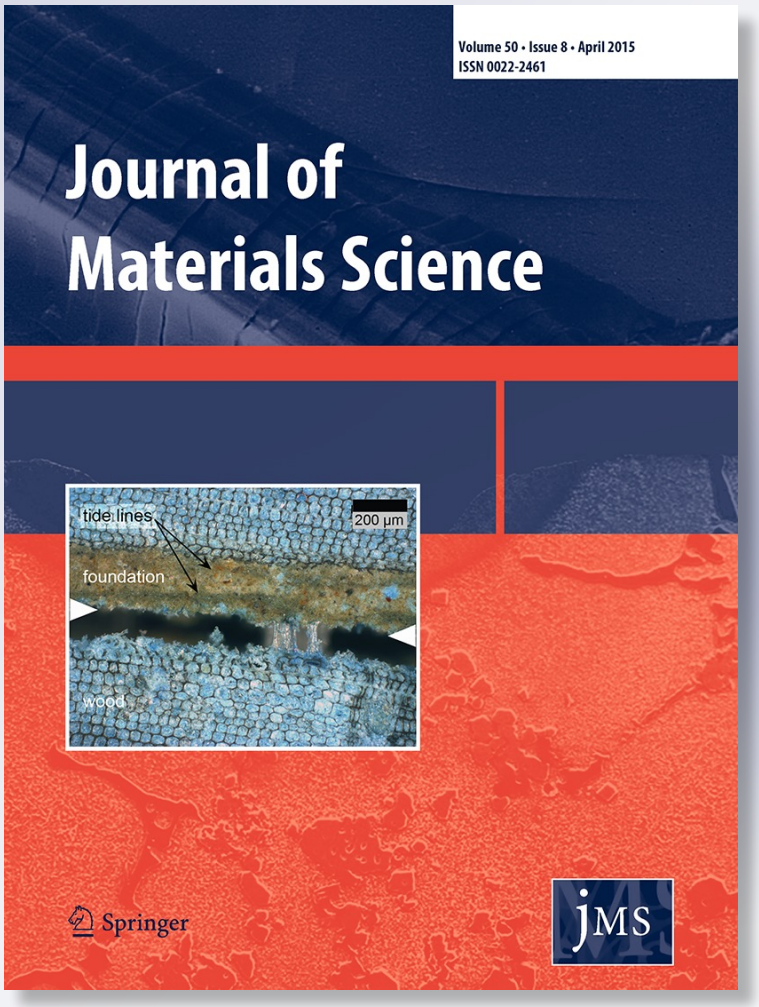


Springer

J Mater Sci (2015) 50:3183–3188
DOI 10.1007/s10853-015-8881-8

# Investigation of Er-doped $Sc_2O_3$ transparent ceramics by positron annihilation spectroscopy

**L. G. Jacobsohn · K. Serivalsatit · C. A. Quarles · J. Ballato**

Received: 2 October 2014 / Accepted: 29 January 2015 / Published online: 7 February 2015


**Abstract** 0.25 at.% Er-doped $Sc_2O_3$ transparent ceramics fabricated using the two-step sintering method with different combinations of sintering temperatures were investigated by positron annihilation spectroscopy. Analysis of the broadening of the annihilation photopeak revealed the presence of the same type of defect in all samples. The lack of long lifetimes ($\tau \geq 2$ ns) suggested no positronium formation or the lack of trapping sites large enough to trap positronium for long enough time for the annihilation to be observed. Analysis of positron annihilation lifetime revealed the presence of a single lifetime that ranged from 208 to 219 ps, depending on the sintering conditions. These results also suggest the absence of a significant presence of vacancy clusters and other larger open-volume defects, and that the dominant open-volume defect corresponds to monovacancies and/or complex defects associated with monovacancies. The bulk lifetime of Er-doped scandia is estimated to be equal or lower than 208 ps.

L. G. Jacobsohn · J. Ballato
Department of Materials Science and Engineering, Clemson University, Clemson, SC 29634, USA

L. G. Jacobsohn (✉) · J. Ballato
Center for Optical Materials Science and Engineering Technologies (COMSET), Clemson University, Anderson, SC 29625, USA
e-mail: luiz@clemson.edu

K. Serivalsatit
Research Unit of Advanced Ceramics, Department of Materials Science, Faculty of Science, Chulalongkorn University, Bangkok, Thailand

C. A. Quarles
Department of Physics and Astronomy, Texas Christian University, Fort Worth, TX 76129, USA

## Introduction

Cubic $Sc_2O_3$ is a promising optical material due to its wide optical transparency window related to a band gap of 5.7 eV that can readily accommodate rare earth dopants spanning emissions from the visible to infrared spectral regions. These properties combined with a high thermal conductivity of 17 W/mK make this material an attractive host for high power solid state lasers [1]. However, in practice, the growth of $Sc_2O_3$ single crystals is difficult, often resulting in small and contaminated specimens [2]. Accordingly, the growth of scandia crystals is an active research topic presently [3]. In order to circumvent crystal growth limitations, Li et al. proposed and fabricated 1-mm-thick transparent ceramics of scandia that reached about 57 % transmittance in the visible region, while estimating the maximum theoretical transmittance to be 79 % [2]. Later, these authors reported improved transmittance of about 70 % [4]. At the same time, Lu et al. reported on continuous wave (CW) laser oscillation from Yb-doped $Sc_2O_3$ transparent ceramics [5]. These reports initiated intense research on the fabrication and application of scandia transparent ceramics as laser gain media and scintillators [6–12].

High temperature sintering allows for the consolidation of powders into dense ceramics below their melting temperature, and recently a method was proposed to decouple densification and crystal growth during sintering [13]. This innovative method was applied to the fabrication of nano/sub-micron-grained transparent ceramics of $Y_2O_3$:Er [10, 14, 15], $Sc_2O_3$:Er [16], $(Tb_{0.8}Y_{0.2})Al_5O_{12}$ [17], and $Lu_2O_3$:Er [18]. Besides the success in achieving high transparency and enhanced mechanical properties [10] using this method, a detailed investigation of the open-volume defects remaining in materials prepared using the

two-step sintering method has not been carried out. The technique of positron annihilation spectroscopy (PAS) is particularly sensitive to the presence of pores with a wide range of sizes. The rate of positron annihilation in matter is a function of the electron density, with lower annihilation rates exhibited by open-volume defects because of the low electron density. PAS has been employed to the characterization of sintered materials, including ZnO [19], yttria-stabilized zirconia [20], porous silica [21], and alumina [22], and in this work it is employed to investigate the effects of different two-step sintering conditions on the porosity of $Sc_2O_3$:Er ceramics for the first time to the best of the authors' knowledge.

## Experimental procedure

The fabrication of $Sc_2O_3$:Er transparent ceramics is only briefly described here as it has been reported in detail elsewhere [16]. Starting nanopowders were prepared by a coprecipitation method in which a scandium nitrate solution was obtained by dissolving $Sc_2O_3$ powder in excess amounts of nitric acid at approximately 80 °C. Erbium nitrate pentahydrate was added into the scandium nitrate solution to yield 0.25 at.% Er-doped scandium nitrate solution. In order to prepare a scandium sulfate solution, Er-doped scandium hydroxide precipitate was first prepared by drop-wise adding a 1.0-M ammonium hydroxide solution into an equivolume amount of 0.2 M Er-doped scandium nitrate solution. Er-doped scandium sulfate was prepared by dissolving the hydroxyl precipitates with a stoichiometric amount of sulfuric acid. The Er-doped $Sc_2O_3$ nanopowders were prepared by adding drop-wise 1.0 M hexamethylenetetramine (HMT) solution into the 0.1-M Er-doped scandium sulfate solution under stirring at 80 °C. After washing and drying, the precursors were calcined at 1100 °C for 4 h under flowing oxygen gas to yield Er-doped $Sc_2O_3$ nanopowders. The calcined nanopowders were uniaxially pressed into pellets at approximately 15 MPa without any binder, followed by cold isostatic pressing at 200 MPa. The two-step vacuum sintering consisted of heating to a higher temperature ($T1$) at a heating rate of 10 °C/min and immediately cooling down to a lower temperature ($T2$) at a cooling rate of 50 °C/min, with the samples being held at $T2$ for 20 h. $T1$ was set at either 1450 or 1500 °C, while $T2$ was varied between 1350 and 1450 °C. In order to obtain transparent ceramics, sintered samples were hot isostatically pressed at 1300 °C under an argon pressure of 206 MPa for 3 h.

The positron annihilation lifetime (PAL) was measured in a typical fast–fast coincidence set-up using two Photonis XP2020/URQ photomultiplier tubes (PMTs) with barium fluoride scintillators [23]. The start and stop signals from the PMTs went to Ortec 583 constant fraction differential discriminators which were set to select the 1.27 MeV gamma ray from the $^{22}$NaCl source for the start signal and the 0.511 MeV annihilation gamma ray for the stop signal. The signals went to an Ortec time-to-amplitude converter and then to an Ortec Trump multi-channel analyzer (MCA) installed in a computer and operated with the software Maestro. The $^{22}$NaCl source, manufactured by Isotope Products Lab., was deposited on 12.5 micron titanium film, and covered and sealed with a second identical titanium film. The source was placed on the one-piece sample and the sample-source was sandwiched between two 1.4-mm titanium foils in order to stop all the positrons from the source. Lifetime runs were made to obtain 1–8 million events total.

The lifetime data were analyzed with the program LT (version 9) [24]. The resolution function was assumed to be two Gaussian functions and the range of data analyzed extended from a counting level about one tenth of the peak to well into the region of the constant random background. The lifetime data were fit with one lifetime component together with a source correction determined using the Monte Carlo code MCNP [25]. The procedure to establish the source correction was to measure the lifetime from the source between the titanium foils alone. The MCNP results were used to determine what fraction of the positron spectrum annihilates in the different parts of the sample-source: the $^{22}$NaCl source, the titanium film covering the source, the sample, and the titanium foil covering the sample and source. In the lifetime data analysis, the contribution from the source consisted of two components, a short component due to both the titanium foil and the $^{22}$NaCl source, and the longer component due to the $^{22}$NaCl source. With the sample-source arrangement used, the contribution to the lifetime spectrum from positrons stopped in the sample was calculated to be 33 %. The MCNP modeling approach for correcting for annihilations in the titanium foil and source was checked by comparing results for two samples of mono-crystalline Si in the conventional two-sample configuration with the case used here of a single sample and titanium foil sandwiching the source. The lifetime results for the Si in the two set-ups agreed within the 2 % statistical error.

The Doppler broadening experiment was done with the same sample-source arrangement, but with the $^{22}$Na source replaced with a $^{68}$Ge source, using a liquid nitrogen cooled high purity germanium detector (HPGe) which is a 5.08-cm coaxial crystal with an aluminum cover. The output signal was processed by an Ortec 571 amplifier and then sent to a second Trump MCA. In the Doppler broadening experiments, data were collected to obtain 4 million events in the 511 keV peak. The analysis of the Doppler broadening spectrum was done with the Sigma Plot software

using an analysis program that analyzes the Doppler broadened 511 keV annihilation gamma ray and determines the S and W parameters for the peak. The S parameter was defined as the ratio of the number of counts within about 1 keV of the 511 peak center to the total number of counts in the peak, while the W parameter corresponded to the ratio of the number of counts in the wings of the peak to the total number of counts in the peak. In the analysis, a step-like background is calculated from the spectrum and subtracted before analysis. No correction has been made for the contribution from positron annihilation in the titanium foils of the source or the titanium substrate.

Optical transmittance measurements was carried out using a Perkin Elmer UV/VIS/NIR Lambda 900 spectrometer at normal incidence. The samples thickness is about 1 mm.

## Results and discussion

Positrons from the $^{22}$NaCl source irradiate all the surface of the sample with an average energy of 182 keV thus probing a region roughly $L_+ = 43$-μm thick, where $L_+$ is the mean penetration depth of the positrons given by $L_+$ (nm) $= 40E_o(\text{keV})^{1.6}/\rho$ (g/cm$^3$) with $E_o$ being the positron energy and $\rho = 3.86$ g/cm$^3$ the material density [26]. Previously, the average grain size of the transparent ceramics was determined to be in the 0.4–0.8 μm range [16], thus data extracted from the PAS measurements are truly representative of the microstructure of the samples as they include the contribution of numerous grains and grain interfaces in addition to open-volume defects. Neglecting annihilation-in-flight that has a very low probability to occur [27], positron annihilation with electrons of the solid occurs after thermalization. Delocalized (during diffusion) and trapped (in an open-volume defect) positrons, as well as positroniums, the unstable self-bonded electron–positron pairs formed when a thermalized positron is captured by an electron, can be annihilated with an electron. Besides the probabilities of formation and trapping, positronium formation also requires sufficiently large open volumes to occur. From these different annihilation mechanisms, delocalized positron annihilation yields the so-called 'bulk' lifetime, while the lifetimes for trapped positron and positronium annihilation are longer and sensitive to the local electron density. As a consequence, the annihilation lifetime is related to the size of the open-volume defect, keeping in mind that because of charge *versus* electrical neutrality considerations for positrons and positroniums, respectively, these species do not usually trap in the same sites depending on the charge state of the open volume related defect.

PAL measurements were carried out and a typical experimental result (open circles) together with its fitting analysis is illustrated in Fig. 1a. The dashed line corresponds to the sample contribution, the dotted and dot-dashed lines correspond to the two components of the source correction as discussed in the previous section, and the continuous line correspond to the best fit to the results. The residual difference between the experimental data and the best fit is shown in Fig. 1b. The results show that the annihilation lifetime distribution is limited to relatively short lifetime values that are as long as about 3 ns. Lack of long lifetimes ($\tau \geq 2$ ns) suggests no positronium formation or the lack of trapping sites large enough to trap positronium for long enough time for the annihilation to be observed. If the lack of positronium formation is assumed to be due to the absence of large enough open-volume defects, then a limit for the maximum defect radius present in these samples can be estimated to be about 3 Å based on the work of Ito, et al. [28]. For the coordination number (CN) 6 of scandia, the ionic radii of $O^{2-}$ and $Sc^{3+}$ are 1.26 and 0.885 Å [29], respectively, suggesting the maximum open-volume defects to be clusters of 2–3 vacancies.

Further analysis of the lifetime data revealed the presence of a single lifetime that ranges from 208 to 219 ps, depending on the sintering conditions, as shown in Fig. 2. This analysis achieved a high degree of confidence with a fit variance ranging from 0.926 to 1.16. Moreover, these results were checked against a two lifetime analysis where

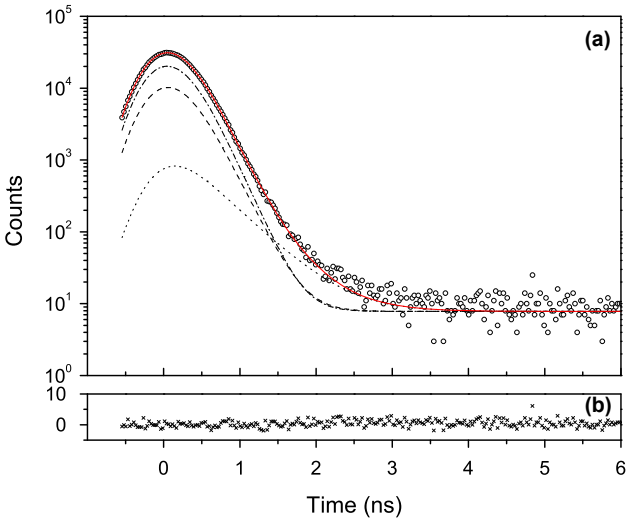


**Fig. 1** PAL results illustrated for sample two-step sintered at $T1 = 1500$ °C and $T2 = 1350$ °C together with deconvolution analysis of the lifetime data. **a** Semi-log plot lifetime distribution up to 6 ns where the experimental results are shown as *open circles*, the best fit as *solid line*, the two source correction components as *dotted* and *dot-dashed lines*, and the sample lifetime as *dashed line*. **b** Linear plot showing the residual difference between the experimental and best fit results

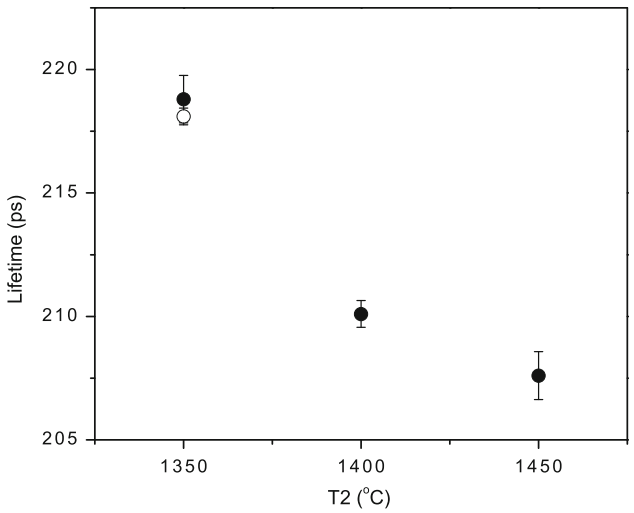


**Fig. 2** Lifetime results of transparent scandia ceramics fabricated with two-step sintering with different conditions as a function of the $T2$ temperature. *Closed symbols* correspond to $T1 = 1500$ °C, and *open symbol* to $T1 = 1450$ °C

the existence of two lifetimes was forced by fixing the value of the faster component assumed to be the bulk lifetime. In most cases, the contribution of the slower component was very low, below 1 %, and was considered unreliable, possibly being an artifact of the fitting procedure. Fits were also done allowing the source contribution to vary. These fits gave essentially the same result with slightly larger errors on the sample lifetime. While the fits obtained in this case were reasonable, it is generally better to fix source contribution to the calculated value since there is otherwise no way to constrain the variation in the fitting program and spurious results could occur when fitting two close values of lifetime. The analysis of the experimental lifetime data has to be considered under the possibility that several unresolved lifetimes exist. The decrease of the lifetime from 219 to 208 ps is interpreted as being due to the decrease of the contribution of positron annihilation in monovacancies and/or monovacancy-related defects due to the consolidation of the ceramic structure induced by higher temperature ($T2$) sintering. This interpretation is in agreement with results reported from PAS characterization of a similar sesquioxide, $Y_2O_3$ [30]. Further support for the elimination of vacancies was obtained from optical transmittance measurements discussed later. The decrease of the lifetime together with the comparison between lifetime values, namely 218 and 219 ps, for samples prepared with $T1 = 1450$ and 1500 °C, respectively, and $T2 = 1350$ °C suggests the second sintering step at $T2$ to control the final pore content. Also, the presence of $Er^{3+}$ (ionic radius = 1.03 Å for CN = 6 [29] ) substituting for $Sc^{3+}$ will distort the lattice and may provide trapping sites for positrons. Based on these results and since no saturation for the lifetime was reached (cf. Fig. 2), the bulk lifetime of Er-doped scandia is estimated to be equal or lower than 208 ps in agreement with the bulk lifetime of $Y_2O_3$, 200 ps [30], and must be understood under the consideration that it may be possible to further lower it using different sintering conditions. These results also suggest the absence of a significant presence of vacancy clusters and other larger open-volume defects.

Additional insight into the defect type was obtained through the analysis of the broadening of the annihilation photopeak. Annihilation of positrons occurs mostly after thermalization and consequently the motion of the electron dominates the relative motion of the electron–positron pair. Since the gamma rays generated in the mutual electron–positron annihilation are Doppler shifted in energy according to the energy of the electron, the broadening of the annihilation photopeak can be related to the nature of the electron. Annihilation with the faster-moving core electrons contributes to the wings of the photopeak, while the slower valence electrons contribute to the central region of the photopeak. The photopeak can be arbitrarily divided in two regions, wings (W) and central (S), with the relative change of these two areas yielding information about the open-volume defects. The S versus W plot is presented in Fig. 3 together with a linear best fit to the data. The fact that a single straight line is capable of representing all the experimental data (within the error bars) suggests that the type of open-volume defect is the same in all samples [23, 31, 32]. Further, the S parameter and lifetime can be correlated in the case of systems with one type of vacancy trapping site such as the one under study here since a larger vacancy trapping site will lead to a larger positron lifetime. A larger trapping site will also lead to lower probability for

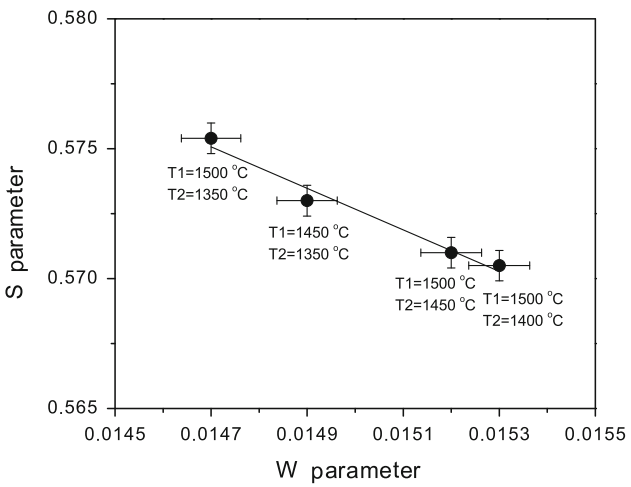


**Fig. 3** S parameter versus W parameter, with each data point obtained from a sample prepared with different two-step sintering conditions. The *line* corresponds to a linear best fit to the data

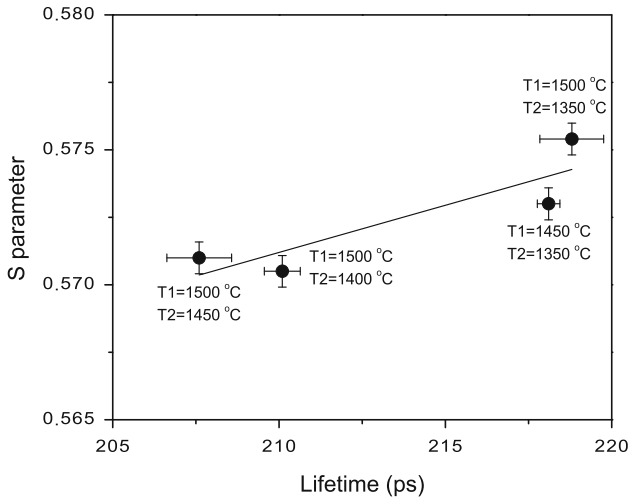


**Fig. 4** S parameter versus lifetime, with each data point obtained from a sample prepared with different two-step sintering conditions. The *line* corresponds to a linear best fit to the data

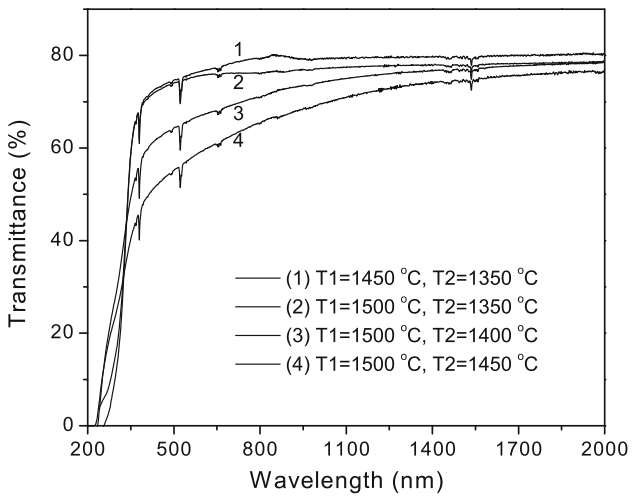


**Fig. 5** Optical transmittance results for samples prepared with different two-step sintering conditions, as indicated

core annihilation and thus to a lower W and a larger S parameters. As can be seen in Fig. 4, the expected correlation in the S parameter and lifetime data is seen supporting the conclusion that as the lifetime and S parameter decrease, the size of the vacancy trapping site or number of such trapping sites decreases.

It is interesting to compare the PAS results with the optical transparency of the ceramics. The optical transmittance of the ceramics is presented in Fig. 5 for all synthesis conditions. The narrow absorption bands at about 380, 522, 654, and 1536 nm are originated in the $Er^{3+}$ dopants [33]. Transmittance is higher for (1) $T1 = 1450$ °C and $T2 = 1350$ °C, and (2) $T1 = 1500$ °C and $T2 = 1350$ °C, with the difference between these spectra being of a few % only, and decreases for higher $T2$ temperatures (with $T1 = 1500$ °C fixed). This trend corresponds to the behavior of the lifetime as a function of $T2$ shown in Fig. 2 and confirms PAS as a useful tool in the characterization of pores in transparent ceramics.

## Summary and conclusions

An investigation of 0.25 at.% Er-doped $Sc_2O_3$ ceramics fabricated using a two-step sintering method with different temperature combinations was carried out by means of PAS. The results suggest that the dominant open-volume defect, at least as detectable by PAS, corresponds to monovacancies and/or complex defects associated with monovacancies. These results confirm PAS to be a useful characterization technique for transparent ceramics. The bulk lifetime of Er-doped scandia is estimated to be equal or lower than 208 ps.

**Acknowledgements** The authors acknowledge financial support from the U.S. Department of Defense Joint Technology Office through their High Energy Laser Multidisciplinary Research Initiative (HEL-MRI) Program for Project ''Eye-Safe Polycrystalline Lasers'' AFOSR Contract # FA9550-07-1-0566. This material is based upon work supported by the National Science Foundation under Grant No. 1207080.

## References

1. Fornasiero L, Mix E, Peters V, Petermann K, Huber G (1999) New Oxide Crystals for Solid State Lasers. Cryst Res Technol 34:255–260
2. Li JG, Ikegami T, Mori T (2003) Fabrication of transparent $Sc_2O_3$ ceramics with powders thermally pyrolyzed from sulfate. J Mater Res 18:1816–1822
3. McMillen CD, Kolis JW (2008) Hydrothermal single crystal growth of $Sc_2O_3$ and lanthanide-doped $Sc_2O_3$. J Crystal Growth 310:1939–1942
4. Li JG, Ikegami T, Mori T (2004) Solution-based processing of $Sc_2O_3$ nanopowders yielding transparent ceramics. J Mater Res 19:733–736
5. Lu J, Bisson JF, Takaichi K, Uematsu T, Shirakawa A, Musha M, Ueda K, Yagi H, Yanagitani T, Kaminskii AA (2003) $Yb^{3+}$:-$Sc_2O_3$ ceramic laser. Appl Phys Lett 83:1101–1103
6. Lupei V, Lupei A, Ikesue A (2005) Transparent Nd and (Nd, Yb)-doped $Sc_2O_3$ ceramics as potential new laser materials. Appl Phys Lett 86:111118
7. Boulon G, Lupei V (2007) Energy transfer and cooperative processes in $Yb^{3+}$-doped cubic sesquioxide laser ceramics and crystals. J Lumin 125:45–54
8. Lupei V, Lupei A, Boulon G, Jouini A, Ikesue A (2008) Cooperative absorption and emission in Yb:$Sc_2O_3$ ceramics. J Alloys Compd 451:179–181
9. Bravo AC, Longuet L, Autissier D, Baumard JF, Vissie P, Longuet JL (2009) Influence of the powder preparation on the sintering of Yb-doped $Sc_2O_3$ transparent ceramics. Opt Mater 31:734–739
10. Serivalsatit K, Kokuoz B, Kokuoz BY, Kennedy M, Ballato J (2010) Synthesis, processing, and properties of submicrometer-

grained highly transparent yttria ceramics. J Am Cer Soc 93:1320–1325
11. Yanagida T, Fujimoto Y, Kurosawa S, Watanabe K, Yagi H, Yanagitani T, Jary V, Futami Y, Yokota Y, Yoshikawa A, Uritani A, Iguchi T, Nikl M (2011) Ultrafast transparent ceramic scintillators using the $Yb^{3+}$ charge transfer luminescence in $RE_2O_3$ host. Appl Phys Exp 4:126402
12. Fukabori A, An L, Ito A, Chani V, Kamada K, Goto T, Yoshikawa A (2012) Scintillation characteristics of undoped $Sc_2O_3$ single crystals and ceramics. IEEE Trans Nuc Sci 59:2594–2600
13. Chen IW, Wang XH (2000) Sintering dense nanocrystalline ceramics without final-stage grain growth. Nature 404:168–171
14. Eilers H (2007) Fabrication, optical transmittance, and hardness of IR-transparent ceramics made from nanophase yttria. J Eur Ceram Soc 27:4711–4717
15. Serivalsatit K, Kokuoz BY, Kokuoz B, Ballato J (2009) Nanograined highly transparent yttria ceramics. Opt Lett 34:1033–1035
16. Serivalsatit K, Ballato J (2010) Submicrometer grain-sized transparent erbium-doped scandia ceramics. J Am Ceram Soc 93:3657–3662
17. Chen C, Zhou S, Lin H, Yi Q (2012) Fabrication and performance optimization of the magneto-optical $(Tb_{1-x}R_x)_3Al_5O_{12}$ (R = Y, Ce) transparent ceramics. Appl Phys Lett 101:131908
18. Serivalsatit K, Wasanapiarnpong T, Kucera C, Ballato J (2013) Synthesis of Er-doped $Lu_2O_3$ nanoparticles and transparent ceramics. Opt Mater 35:1426–1430
19. Fernández P, de Diego N, del Río J, Llopis J (1989) A positron study of sintering processes in ZnO-based ceramics. J Phys 1:4853–4858
20. Yagi Y, Hirano S, Ujihira Y, Miyayama M (1999) Analysis of the sintering process of 2 mol % yttria-doped zirconia by positron annihilation lifetime measurements. J Mater Sci Lett 18:205–207
21. Yu-Yang H, Chao X, Yu-Xin W, Yan-Qiong L, Wen D (2009) Influence of sintering temperature on defects in porous silica monoliths studied by positron annihilation techniques. Mater Sci Forum 607:204–206
22. Djourelov N, Aman Y, Berovski K, Nédélec P, Charvin N, Garnier V, Djurado E (2011) Structure characterization of spark plasma sintered alumina by positron annihilation lifetime spectroscopy. Phys Status Solidi A 208:795–802
23. Prochazka I (2001) Positron annihilation spectroscopy. Materials. Structure 8:55–60
24. Kansy J (1996) Microcomputer program for analysis of positron annihilation lifetime spectra. Nucl Instr Meth Phys Res A 374:235–244
25. Urban-Klaehn M, Spaulding R, Hunt AW, Peterson ES (2007) Phys Stat Sol C 4:3732–3734
26. Schultz PJ, Lynn KG (1988) Interaction of positron beams with surfaces, thin films, and interfaces. Rev Mod Phys 60:701–779
27. Asoka-Kumar P, Lynn KG, Welch DO (1994) Characterization of defects in Si and $SiO_2$-Si using positrons. J Appl Phys 76:4935–4982
28. Ito K, Nakanishi H, Ujihira Y (1999) Extension of the equation for the annihilation lifetime of ortho-positronium at a cavity larger than 1 nm in radius. J Phys Chem B 103:4555–4558
29. Shannon RD (1976) Revised effective ionic radii and systematic studies of interatomic distances in halides and chalcogenides. Acta Crystallogr A 32:751–767
30. Brown J, Mascher P, Kitai AH (1995) Positron lifetime spectroscopy and cathodoluminescence of polycrystalline terbium-doped yttria. J Electrochem Soc 142:958–960
31. Saarinen K, Hautojarvi P, Corbel C (1998) Identification of defects in semiconductors. In: Stavola M (ed) Semiconductors and Semimetals, vol 51A. Academic Press, San Diego, p 209
32. Jacobsohn LG, Nastasi M, Daemen LL, Jenei Z, Asoka-Kumar P (2005) Positron annihilation spectroscopy of sputtered boron carbide films. Diamond Rel Mater 14:201–205
33. Gheorghe C, Georgescu S, Lupei V, Lupei A, Ikesue A (2008) Absorption intensities and emission cross section of $Er^{+3}$ in $Sc_2O_3$ transparent ceramics. J Appl Phys 103:083116